 doi:10.20944/preprints202104.0270.v1

Barriers to small molecule drug discovery for systemic amyloidosis

Gareth J Morgan*

Amyloidosis Center and Department of Medicine, Section of Hematology and Medical Oncology, Boston University School of Medicine, Boston, MA 02118

*Correspondence: gjmorgan@bu.edu +1-617-358-4743

Abstract

Inhibition of amyloid fibril formation could benefit patients with systemic amyloidosis. In this group of diseases, deposition of amyloid fibrils derived from normally soluble proteins leads to progressive tissue damage and organ failure. Although many small molecules have been proposed as inhibitors of amyloid formation, few have been successful in clinical trials. Amyloid formation is complex and several individual steps could be targeted by small molecules. However, the exact mechanism of action for a molecule is often not known, which impedes medicinal chemistry efforts to develop more potent molecules. Furthermore, commonly used assays are prone to artifacts that must be controlled for. Here, potential mechanisms by which small molecules could inhibit aggregation of immunoglobulin light chain dimers, the precursor proteins for AL amyloidosis are studied in assays that recapitulate different aspects of amyloidogenesis in vitro. One molecule reduced unfolding-coupled proteolysis of light chains, but no molecules inhibited aggregation of light chains or disrupted pre-formed amyloid fibrils. This work demonstrates the challenges associated with drug development for amyloidosis, but also highlights the potential to combine therapies that target different aspects of amyloidogenesis.

Keywords

Systemic amyloidosis; amyloid fibrils; amyloidogenesis inhibitors; antibody light chains; light chain stabilizers; doxycycline; EGCG; thioflavin T; filter trap; PAINS

Preprints (www.preprints.org) | NOT PEER-REVIEWED | Posted: 9 April 2021 doi:10.20944/preprints202104.0270.v1

1. Introduction

Deposition of amyloid fibrils derived from antibody light chain (LC) proteins is associated with organ damage in the disease amyloid light chain (AL) amyloidosis [1,2]. AL amyloidosis is the most commonly diagnosed form of “systemic” amyloidosis, where amyloid fibrils form in multiple tissues [3]. In these diseases, amyloid fibrils are closely associated with pathology, and inhibition of amyloid deposition by suppression or stabilization of the precursor protein can lead to clinical benefit [4]. Here, I use “amyloidosis” to refer to the disease and “amyloidogenesis” to mean the biochemical process of amyloid formation from soluble precursor proteins. “AL” is often used as a shorthand for AL amyloidosis, but strictly refers to the amyloid protein in its fibrillar state [3].

In AL amyloidosis, the precursor LCs are secreted from a clonal population of B lymphocytes, most often plasma cells in the bone marrow [1]. Amyloid fibrils are formed from a single “monoclonal” LC with a sequence that is unique to each patient. LCs are ~215-residue proteins that form two structural immunoglobulin domains. The N-terminal variable (V_L) domain, which forms the structured core of AL amyloid fibrils, is the location of most of the diversity between LCs. The C-terminal constant (C_L) domain is much more conserved and has a scaffolding and chaperone function. LCs can form homodimers, as shown in Figure 1.

Preprints (www.preprints.org) | NOT PEER-REVIEWED | Posted: 9 April 2021 doi:10.20944/preprints202104.0270.v1

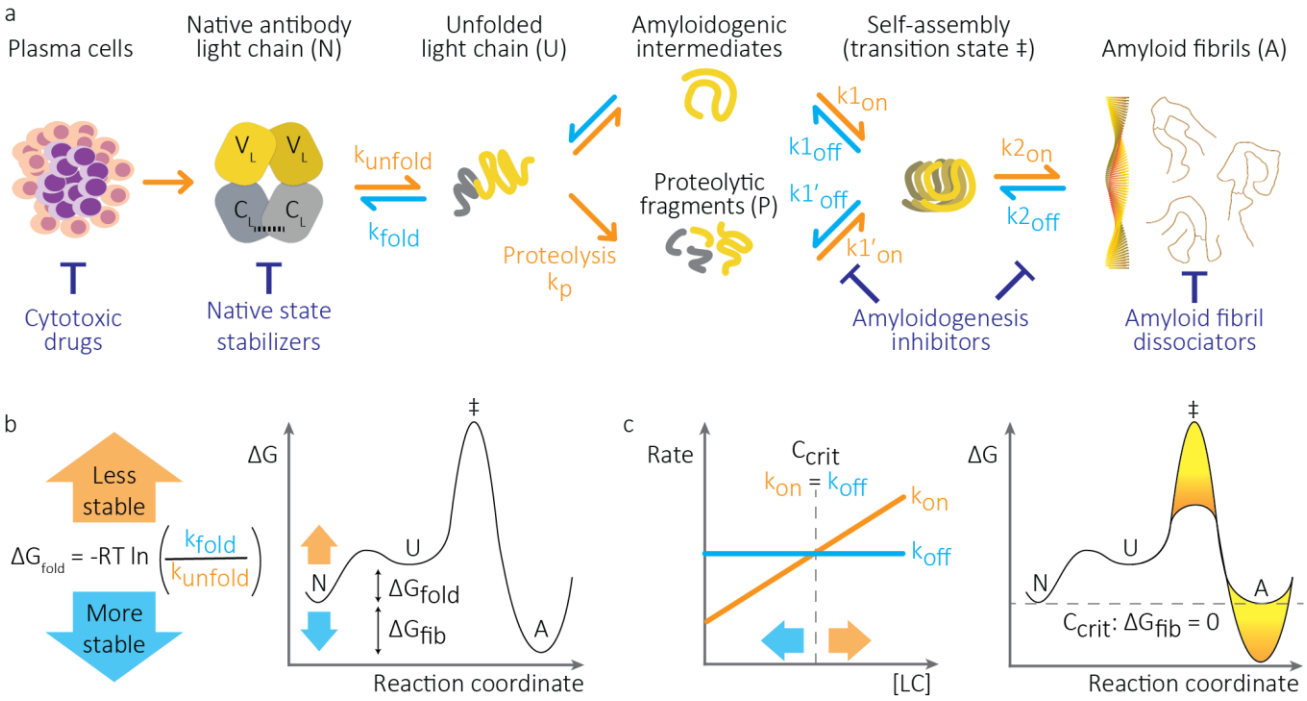

Figure 1: Amyloid formation by antibody light chains. (a) In AL amyloidosis, LCs, shown here as a homodimer, are secreted from a clonal population of plasma cells. Once in circulation, LCs can unfold to amyloid-competent structural states, which may involve proteolysis. Inter-molecular interactions within this population of non-native structures can lead to the formation of polymeric species including amyloid fibrils. Processes that lead to amyloid formation are shown as orange arrows, while those which antagonize amyloidogenesis are shown as blue arrows. Reversible processes are shown as equilibria. Reaction rates for these processes can in some cases be calculated. The folding and unfolding rate constants of the native LC are defined as k_{fold} and k_{unfold}, respectively. The self-assembly process is divided into initiation and elongation steps, with rate constants $k1_{on/off}$ and $k2_{on/off}$, respectively. Proteolysis is irreversible with a rate constant of k_p and leads to self-assembly of fragments with rate constants $k1'_{on/off}$. LCs can form multiple fibril structures. Structures of the peptide backbone conformation observed within three LC amyloid fibrils (clockwise from top: PDB codes 6Z1I, 6HUD and 6IC3) are shown, oriented by the intramolecular disulfide bond within the V_L-domain. Therapies for AL amyloidosis (shown with flat-ended blue lines) could potentially target any of these steps, which implies that combining therapies with different mechanisms of action could benefit patients. Existing treatments aim to kill the clonal cells that secrete the LCs. Alternative treatments could suppress formation of non-native amyloidogenic LC species (stabilizers); inhibit self-association (amyloidogenesis inhibitors) or promote the dissolution or removal of existing fibrils (amyloid fibril dissociators). (b) The role of LC native state stability in amyloidogenesis. Amyloidogenic LCs appear to be less stable than other LCs, in terms of the population of non-native states at equilibrium and the frequency at which an individual protein unfolds. The equilibrium stabilities of native LCs and amyloid fibrils are defined as ΔG_{fold} and ΔG_{fib},

Preprints (www.preprints.org) | NOT PEER-REVIEWED | Posted: 9 April 2021 doi:10.20944/preprints202104.0270.v1

respectively. (c) Concentration dependence of the equilibrium between soluble and aggregated protein. At higher concentrations (darker orange shading on the energy landscape), the rate of aggregate formation increases while the rate of aggregate dissociation remains constant. The result is a reduced energy barrier to protein aggregation and an increased proportion of aggregated protein at equilibrium. At the critical concentration, C_{crit}, shown by a dashed line, the on- and off-rates, $k_{on/off}$, are equal, and the free energy difference between soluble and aggregated protein is zero.

Preventing amyloid deposition in AL amyloidosis is a longstanding goal of research and treatment. Cytotoxic chemotherapy can kill the clonal plasma cells, thus reducing levels of monoclonal LCs below that necessary for aggregation. An array of molecules are used in clinical practice, all originally developed for the related cancer, multiple myeloma [5]. Most drugs are used off-label. The first specific approval for AL amyloidosis by the US FDA, of the CD38-directed monoclonal antibody daratumumab [6], was granted in January 2021. However, many patients are diagnosed after the onset of organ failure, which complicates treatment [7]. Therefore, substantial efforts are devoted to developing therapeutic strategies that could benefit these patients [8].

Amyloidogenesis by folded proteins is a complex, multi-step process (Figure 1), and pharmacologic intervention at any of these points could potentially benefit patients. Importantly, these steps could be targeted in combination, which could potentially lead to synergy between approaches. Unfortunately, this complexity makes it difficult to identify how a small molecule may prevent aggregation. Such uncertainty is a barrier to rational development of highly efficacious drug candidates.

In order for LCs to form amyloid fibrils, productive interactions must occur between rare, transiently populated LC structural species. The steady-state concentration of these species is defined by both the rate of LC secretion from plasma cells and the stability of the LC, which is its propensity to remain in its folded state. Post-translational modifications may alter these processes. Most clearly, proteolytic cleavage of LCs can lead to fragments which are more amyloidogenic [9,10]. Full-length LCs are more stable in vitro and less prone to aggregation under native-like conditions than their component V_L-domains [9,11]. AL fibrils appear to be primarily composed of fragments of LCs, although the nature of this cleavage is unknown and may happen after deposition as amyloid [10,12–16]. The nascent amyloid fibrils must be stable enough to recruit new protein molecules and grow into mature fibrils, rather than dissociate. These fibrils deposit in tissues and form interactions with other molecules such as components of the extracellular matrix and the protein serum amyloid P component (SAP), which further stabilizes them. Finally, fibrils must be resistant to clearance by

cells including macrophages that would normally remove macroscopic debris. The fine details of how these processes play out in an individual patient likely depend on the unique sequence of the monoclonal LC.

Other than eradication of the producer cells, there are several potential mechanisms by which a drug could benefit individuals with AL amyloidosis. One strategy is to suppress unfolding of the protein and thereby reduce the levels of amyloid-competent species. This approach has been clinically efficacious in transthyretin amyloidosis, where the “kinetic stabilizer” drug tafamidis is approved in multiple regions [17,18]. Other molecules that act as kinetic stabilizers include the anti-inflammatory drug diflunisal [19,20], the Parkinson’s disease drug tolcapone [21], and the investigational molecule AG10 [22]. Several molecules have been proposed as stabilizers of LCs [23–25] and we are actively pursuing this strategy. Alternatively, a drug could interfere with the self-association of non-native amyloid precursors to suppress self-association and amyloid formation. This approach has been explicitly pursued for α-synuclein [26], and is proposed as a mechanism of action of other molecules. A similar approach is the capping of pre-existing amyloid fibrils to prevent their extension [27]. A third group of potential therapies aims to dissociate pre-existing amyloid fibrils, either via small molecules, antibodies, or a combination of the two. The most advanced therapies have used monoclonal antibodies directed at either the fibrils themselves [28,29] or the accessory protein SAP [30,31] to recruit phagocytic cells to clear the amyloid. At the time of writing, Phase 3 studies of two anti-amyloid monoclonal antibodies, known as NEOD001 and CAEL101, are in progress [28,29].

A wide variety of small molecules have been suggested as potential therapies for different amyloid diseases. Several small molecules have shown some efficacy in in vitro assays of amyloidogenesis, or even in clinical trials, but intense lead optimization has not generally been carried out. The action of drug-like small molecules on amyloidogenesis is often assessed by their ability to prevent amyloid formation in vitro. However, molecules could in principle act anywhere along the reaction pathway depicted in Figure 1. More problematically, experimental artifacts could occur at any point along this pathway.

One potential therapeutic in AL amyloidosis is doxycycline. This widely-prescribed tetracycline antibiotic has been shown to prevent amyloidogenesis and disrupt amyloid fibrils formed by several proteins in vitro [32–34]. Doxycycline suppressed amyloid deposition in a mouse model of AL amyloidosis [34] and reduced toxicity in a nematode model [35]. Clinical studies have shown a beneficial effect of using doxycycline over other antibiotics in patients with AL amyloidosis [36–38]. Although these effects are generally described as being due to doxycycline’s ability to disrupt amyloid fibrils, doxycycline is a pleiotropic molecule that could affect many aspects of amyloid formation or patient metabolism. For example, tetracyclines are inhibitors of translation [39] and of

matrix metalloproteinases [40], which may both contribute to efficacy. Alternatively, doxycycline could simply be an effective antibiotic in patients with amyloidosis, which is potentially important since treatments directed at antibody-secreting cells can have severe immunosuppressive side effects.

Another molecule that has been studied in detail is epigallocatechin gallate (EGCG), a bioactive compound found in green tea. Biochemical studies show that EGCG can modulate protein aggregates, in some cases “remodeling” fibrils to form other oligomeric species [41,42]. However, a Phase 2 trial of EGCG in AL amyloidosis failed to show significant benefit [43] and two other trials (NCT01511263 and NCT02015312) have not reported results.

Although doxycycline, EGCG and other molecules could have real, beneficial activity in AL amyloidosis, the mechanisms by which they might exert such activity are poorly understood. Deeper understanding of these mechanisms could lead to more effective use of these and other molecules. It is possible to envision combination therapies that use cytotoxic agents to kill clonal cells, molecules that suppress aggregation to suppress non-native LCs, and strategies that enhance clearance of amyloid.

Small molecules that prevent amyloid formation in vitro could potentially act via at least three mechanisms: inhibiting unfolding or proteolysis of LCs to form amyloid-competent structures; inhibiting self-association of non-native LCs; and enhancing dissociation or dissolution of pre-formed amyloid fibrils. To distinguish between potential mechanisms of action, multiple assays that isolate specific steps in the process must be considered. Here, I asked whether small molecules demonstrate activity in simple assays of LC stability and aggregation. These assays do not fully recapitulate the process of amyloidogenesis in vivo, and natural products or screening molecules would not be expected to show high potency in an initial screen. However, true-positive activity in one or more of these assays, confirmed by an orthogonal assay, would be a reasonable basis for starting a drug development program from a screening hit.

Eight molecules were studied (Figure 2). (1) Coumarin 1, which was identified as a stabilizer of native LCs [23]. (2) Doxycycline, which has been proposed to inhibit amyloid formation by several proteins and disrupt amyloid fibrils [32,33,44]. (3) Oxidized and (4) reduced forms of EGCG (EGCGox and EGCGred, respectively), which have been proposed to remodel amyloid fibrils [41,42]. (5) Rifampicin and (6) rifamycin SV, two related antibiotics. These molecules have been shown in vitro to interfere with self-association of ß2-microglobulin, an amyloid forming protein with a C_L-domain-like secondary structure [45]. (7) Methylene blue, which has been shown to inhibit formation of amyloid fibrils by tau [46] and light chains [25]. (8) Diflunisal, a stabilizer of the native

Preprints (www.preprints.org) | NOT PEER-REVIEWED | Posted: 9 April 2021 doi:10.20944/preprints202104.0270.v1

state of transthyretin [19,20] is not expected to interact with LCs and was included as a negative control.

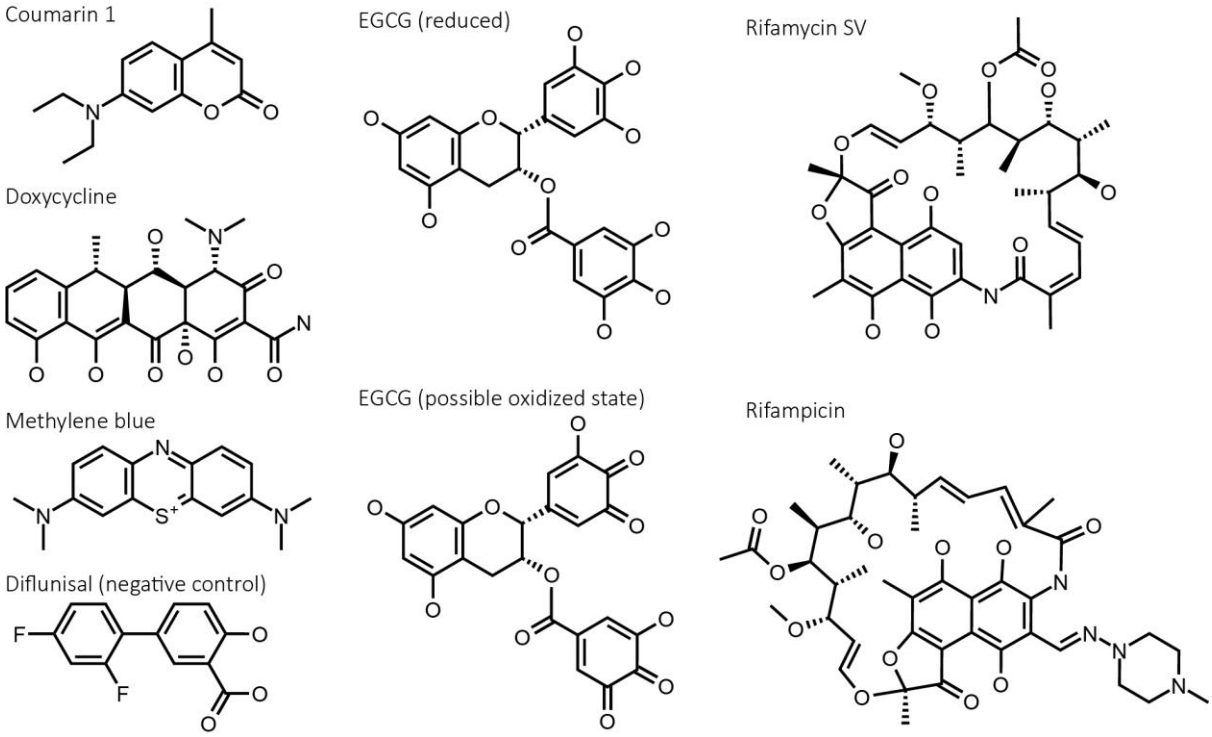

Figure 2: Structures of small molecules used in this study. The natural product EGCG can undergo oxidation to form reactive orthoquinone species such as that shown. To generate these species, I incubated EGCG solutions for 24 h at 37 °C. Diflunisal, a stabilizer of transthyretin, is not expected to interact with LCs and is included as a negative control.

2. Results

I investigated three potential mechanisms of action for small molecules: native state stabilization, using the full-length LC; inhibition of V_L-domain amyloidogenesis; and dissolution of pre-formed V_L-domain amyloid fibrils. I used LCs derived from the IGLV6-57 gene, which is over-represented in AL amyloidosis [47]. For each experiment, a different LC was used in order to maximize the signal that was measured, as described below. In all experiments, LC concentration was 5 μM (monomer equivalent; 0.06 mg/ml V_L-domain or 0.12 mg/ml full-length LC) and small molecule concentration was 50 μM. All experiments were carried out in phosphate buffered saline at pH 7.4 and 37 °C. Doxycycline, EGCG and methylene blue are soluble in water at the stock concentration of 5 mM; other molecules were dissolved in ethanol. To verify that the ethanol had no influence on the LCs, additional controls using 1% (v/v) ethanol vehicle were used in each experiment.

Preprints (www.preprints.org) | NOT PEER-REVIEWED | Posted: 9 April 2021 doi:10.20944/preprints202104.0270.v1

2.1. Native state stabilization

Amyloid fibrils are non-native assemblies and many studies have shown that unfolding from the LC native state is required for amyloid formation. The rate at which LCs unfold to form non-native species is described by their kinetic stability, which describes the energy barrier to unfolding. To efficiently measure kinetic stability, I used limited proteolysis [48]. Non-native LC conformations are more susceptible to endoproteolysis than native LCs because endoproteases preferentially bind to unstructured peptide substrates. Because proteolysis is irreversible, the rate at which a folded protein is degraded is determined by its unfolding rate, a situation known as EX1 kinetics. Stabilization was assessed using an unstable full-length LC derived from a patient with AL, known as WIL, which we previously showed could be stabilized by small molecules [23]. I used this unstable LC to maximize the potential signal of the experiment, which is defined by the extent to which unliganded LCs are degraded over the incubation period. This approach of using a single timepoint measurement to infer the kinetics of a well-defined system is a way to minimize the number of measurements required for an experiment, which is important for high-throughput screening.

LCs were incubated with proteinase K, a highly active protease that cleaves after aliphatic residues. Using this protease allows for detection of transient unfolding of regions of LCs that lack may cleavage sites for a less promiscuous protease. Three replicates were measured. After 4 h incubation at 37 °C, reactions were quenched with a covalent protease inhibitor and residual full-length LC measured by SDS-PAGE. The extent of degradation of LCs in the presence or absence of small molecules is shown in Figure 3. Of the molecules tested, only coumarin 1 consistently protected the LC against proteolysis, consistent with the results of a previous high-throughput screen [23].

Preprints (www.preprints.org) | NOT PEER-REVIEWED | Posted: 9 April 2021 doi:10.20944/preprints202104.0270.v1

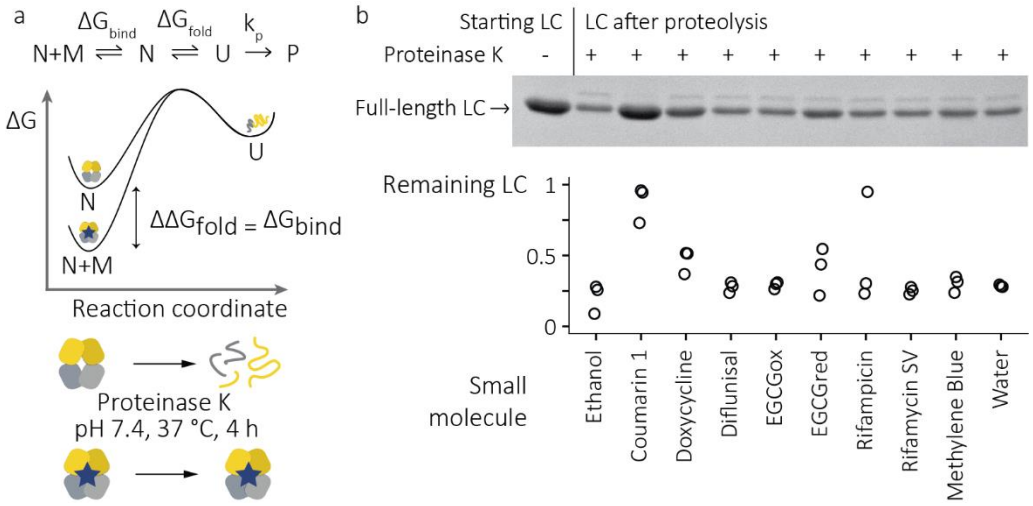

Figure 3: Stabilization of LCs measured by proteolysis. A) Experimental outline. Transient unfolding of LCs to protease-sensitive conformations limits the rate at which the LCs are cleaved by proteinase K. Binding of small molecule ligands (shown as blue stars) stabilizes LCs against unfolding and therefore reduces the rate of proteolysis. N, native state; M, small molecule, U, unfolded state; P, proteolytically degraded state. B) Residual full-length LC after incubation with proteinase K and small molecules was measured by SDS-PAGE (n = 3 independent reactions per molecule). Top, example gel showing the starting material (left lane) and remaining LC after incubation (right lanes). Bottom, quantitation of gel bands, relative to the unproteolyzed LC.

2.2. Inhibition of aggregation

Almost all peptide sequences can form amyloid fibrils under some set of conditions. Amyloid fibrils are often described as the most stable state for a protein, and amyloid formation is sometimes regarded as “irreversible”. However, fibrils and soluble protein exist in equilibrium, so amyloid is only the most stable conformation at concentrations above the critical concentration (C_{crit}) or solubility limit (Figure 1C). This limit can be thought of as the concentration at which protein molecules associate and dissociate from the fibril at equal rates. Association rates (k_{on}) are determined by the frequency at which soluble protein molecules collide with the fibril ends and are therefore concentration dependent, typically second-order or higher. Dissociation rates (k_{off}) are determined by the stability of the interactions within the fibrils, which are not dominated by the size of the fibril and are therefore less concentration dependent.

Preprints (www.preprints.org) | NOT PEER-REVIEWED | Posted: 9 April 2021 doi:10.20944/preprints202104.0270.v1

Initiation of amyloid formation depends on productive interactions between high-energy intermediates to form a nucleus that is more stable than the precursors. However, once this nucleus is formed, addition of further protein molecules is more rapid because, compared to the unfolded species, the nucleus is long-lived. This can be visualized as a reduced energy barrier to amyloid formation in the presence of pre-formed seeds (Figure 1). Extension is therefore more rapid than initiation in terms of numbers of molecules added per unit time.

This simple model is a useful framework for thinking about how small molecules could inhibit amyloidogenesis. Small molecules that alter the unfolded protein conformational ensemble or inhibit self-association could suppress aggregation via multiple mechanisms, such as those shown in Figure 4. However, rational design of such molecules is difficult because the properties of the protein species that self-assemble are not known, and these species are only transiently present in solution, often at very low concentration. Efforts to identify inhibitors of amyloidogenesis therefore often rely on screening libraries of compounds with assays that detect amyloid fibril formation. The most common assay is to measure the fluorescence of thioflavin T (ThT), a benzothiazole dye with environment sensitive fluorescence properties. The fluorescence emission of ThT increases when the molecule binds to amyloid fibrils, so loss of this fluorescence signal is associated with inhibition of amyloidogenesis. However, these assays are prone to false positives because displacement of ThT from fibrils or quenching of fluorescence could be interpreted as inhibition of amyloid formation (Figure 4). Furthermore, the emission of fibril-bound ThT is not well understood and differs between batches of fibrils. Such experiments should be validated using an orthogonal assay, such as monitoring loss of soluble protein. Aggregation often proceeds with “sigmoidal” kinetics where a “lag” phase is followed by a rapid increase in ThT fluorescence. Molecules that extend the lag phase may be more likely to be true positive hits than those that reduce the final fluorescence intensity of the aggregate-bound ThT. A number of molecules have been proposed to alter the morphology of the aggregates formed in vitro. However, since the mechanisms by which amyloid fibrils cause tissue damage are poorly understood, it is not clear whether species such as “spherical oligomers”, “amorphous aggregates” or “protofibrils” actually represent a less toxic endpoint than amyloid.

Preprints (www.preprints.org) | NOT PEER-REVIEWED | Posted: 9 April 2021 doi:10.20944/preprints202104.0270.v1

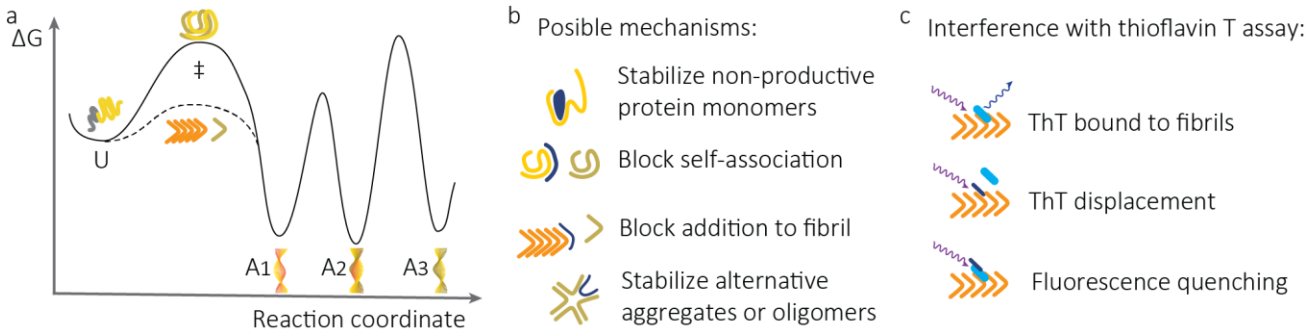

Figure 4: Amyloid formation by non-native LCs. (a) Schematic energy landscape. The endpoint proportion of aggregated LCs is defined by the critical concentration, but the rate at which this reaction proceeds is determined by the self-association of amyloid-competent non-native LCs. Multiple fibril structures may be accessible to the LCs, shown as three energy minima. However, the energy barriers to interconversion between these states are likely to be large, requiring dissociation, unfolding and reaggregation of the subunit molecules. (b) Small molecules could inhibit amyloid formation (or enhance amyloid dissociation) via multiple mechanisms, depicted schematically. (c) Amyloid formation can be readily measured by binding of the fluorogenic dye thioflavin T (shown as a cyan bar), but small molecules (black bars) may interfere with this assay. Excitation and emission photons are shown as wavy arrows.

To ask whether small molecules can inhibit amyloidogenesis, I measured their effect on the aggregation of a LC V_L-domain that reproducibly forms amyloid fibrils in vitro, known as JTO-V_L (Figure 5) [49]. Full-length LCs derived from the IGLV6-57 gene, including JTO, do not readily aggregate at neutral pH, but their isolated V_L-domains do so. JTO-V_L is not derived from a patient with amyloidosis, but it aggregates readily and is predominantly folded under the conditions used for aggregation [9,50]. I reasoned that its native-state stability would allow detection of changes in aggregation rate due to small molecule modulation of the unfolded state ensemble. As a negative control, I used full-length JTO, which does not exhibit a change in ThT fluorescence under similar conditions [9,51].

Preprints (www.preprints.org) | NOT PEER-REVIEWED | Posted: 9 April 2021 doi:10.20944/preprints202104.0270.v1

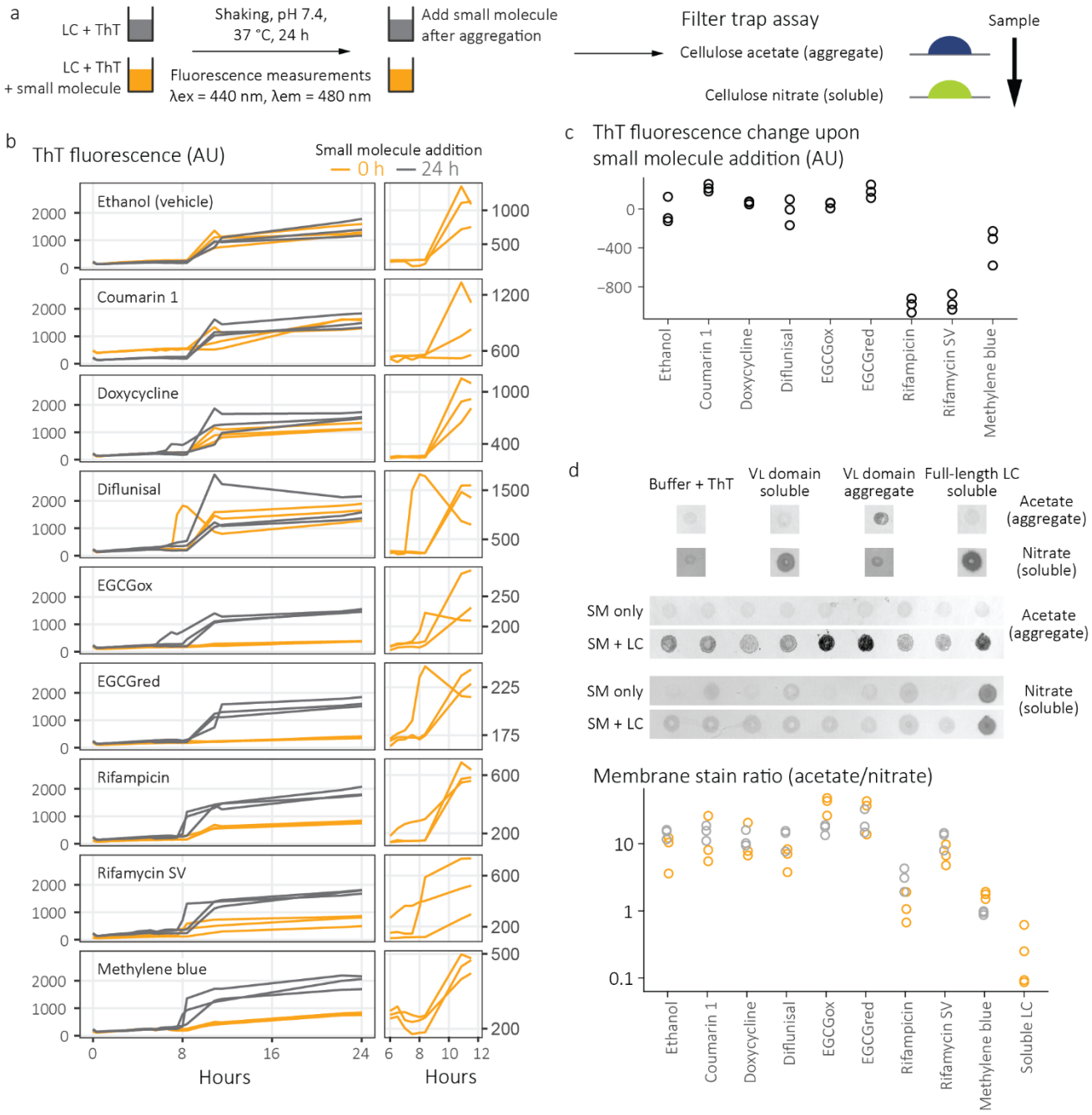

Figure 5: Aggregation of LC VL-domains measured by thioflavin T fluorescence and filter trap assay. (a) Experimental design. After 24 h of aggregation monitored by ThT fluorescence, the effect of small molecule addition to pre-formed fibrils on ThT fluorescence was measured, and the amount of soluble and aggregated LC is quantitated by filter trap assay. (b) Aggregation kinetics measured by ThT fluorescence. Orange traces represent fluorescence intensity changes (n = 3 wells) in the presence of small molecules; grey traces represent control wells where small molecules were added after 24 h (n = 3 wells). Panels on the right show the detail of the time period where aggregation occurs. (c) The effect of addition of small molecules to pre-formed, ThT-bound fibrils was measured. The decrease in ThT fluorescence shown for rifampicin, rifamycin SV and methylene blue is

Preprints (www.preprints.org) | NOT PEER-REVIEWED | Posted: 9 April 2021 doi:10.20944/preprints202104.0270.v1

consistent with fluorescence quenching or displacement of ThT from fibrils. (d) Quantitation of soluble and aggregated LCs by filter trap assay. Control samples (top) show the staining of soluble or aggregated LCs on cellulose acetate or cellulose nitrate membranes. Two types of soluble LCs were used as negative controls for aggregation: JTO-V_L that had not been incubated at 37 °C and full-length JTO that did not aggregate over the course of the experiment. Example membrane regions are shown below. Note that several small molecules, especially methylene blue, stain the membranes in the absence of protein, which affects their apparent quantitation. At bottom, the ratios of aggregated to soluble LCs are shown for each individual sample. Orange points represent wells where small molecules were present throughout the aggregation process; grey points represent wells where the small molecules were added after aggregation had occurred.

To minimize variation between samples, I carried out all the aggregation reactions in parallel on the same microwell plate. In the absence of small molecules, JTO-V_L reproducibly forms ThT-binding aggregates after 8-12 h of incubation with continuous shaking (Figure 5B). Both oxidized and reduced EGCG, rifampicin and rifamycin SV, and methylene blue all suppress the rise in ThT fluorescence associated with amyloidogenesis. However, closer examination of the kinetic traces (Figure 5B, right panels) reveals an increase in ThT fluorescence at a similar time to that observed in the absence of small molecule. To test whether these molecules disrupt the binding or fluorescence of ThT, additional samples of JTO-V_L in adjacent wells were allowed to aggregate for 24 h, after which small molecules were added. The change in ThT fluorescence upon addition of rifamycin SV, rifampicin and methylene blue is consistent with suppression of ThT fluorescence, rather than inhibition of aggregation (Figure 5C).

At the endpoint of the aggregation reactions, the presence of soluble and insoluble LC aggregates was assessed by a “filter trap” differential membrane binding assay [52]. Samples are drawn through a cellulose acetate membrane, which traps large aggregates, then a cellulose nitrate membrane, which binds soluble protein. Protein binding to each membrane is measured by staining with amido black dye [53]. Molecules which suppress aggregation would be expected to reduce the amount of insoluble protein and retain soluble protein. In each case, staining of soluble LCs decreased substantially compared to the non-aggregated controls, consistent with the presence of aggregates. Several molecules, particularly methylene blue, are colored, and cause visible staining on one or both membranes, making quantitation difficult. Despite this limitation, Figure 4D shows that aggregated LC species are present in all samples.

Preprints (www.preprints.org) | NOT PEER-REVIEWED | Posted: 9 April 2021 doi:10.20944/preprints202104.0270.v1

These data indicate that none of the small molecules tested prevent LC VL-domain aggregation under these conditions. It is possible that non-amyloid aggregates are formed, which do not bind to ThT, but soluble protein is not retained in solution.

2.3. Dissolution of pre-formed amyloid fibrils

Above the critical solubility concentration, amyloid fibrils are more stable than their soluble precursors. Molecules that preferentially bind to amyloid fibrils over native LCs would enhance the stability of the fibrils and suppress dissolution. Conversely, stabilization of non-fibrillar species could increase C_{crit} and enhance fibril dissolution. A small molecule could suppress the formation of amyloid fibrils and also disaggregate fibrils by these mechanisms, since they are equivalent in the simple equilibrium model shown in Figure 4. An exception to this principle is small molecules that covalently bond to LCs to form a less amyloidogenic product. A small molecule which preferentially reacts with fibrillar protein may have only a small effect on aggregation rates, but given time and a high local concentration of fibrils could lead to fibril dissociation via a unidirectional “molecular ratchet” mechanism. In this scenario, the relatively high concentration of fibrillar protein could yield a high enough reaction rate to resolubilize the fibril via an EX1 mechanism, whereas a reactive conformation within a pre-fibrillar structural ensemble may not be present for long enough to react. Covalent modification of proteins has been proposed as a mechanism by which EGCG can “remodel” amyloid fibrils [42].

To investigate these potential mechanisms, I formed LC V_L-domain amyloid fibrils from a relatively stable V_L-domain, the “germline” *IGLV6-57* sequence, referred to as 6aJL2-V_L [54]. I used this V_L-domain to maximize the likelihood that any LC that dissociated from the fibril would remain folded in solution. Amyloid dissolution is likely to occur slowly because of the large free energy barrier to dissociation (Figure 1B, moving from right to left across the energy landscape). Doxycycline has been reported to dissociate amyloid fibrils over a 15-day time period. Therefore, I asked whether duplicate fibril samples had dissociated to soluble material after 7 or 15 days of incubation with small molecules.

After 7 and 15 days of incubation at 37 °C, LC solubility was assessed by filter trap assay (Figure 6). To maximize the detection of soluble or insoluble material, LCs were precipitated by centrifugation, and the supernatant and resuspended precipitate were analyzed separately for each time point (orange and blue symbols in Figure 6, respectively). A single sample of soluble LC was used as a positive control. Staining of membranes by small molecules impeded quantitation of solubility, as described above. The proportion of aggregated LC can be inferred from the ratio of cellulose acetate staining to cellulose nitrate staining (Figure 6C), which shows no difference between samples incubated with or without any small molecule except for methylene blue. However,

Preprints (www.preprints.org) | NOT PEER-REVIEWED | Posted: 9 April 2021 doi:10.20944/preprints202104.0270.v1

methylene blue preferentially stains cellulose nitrate (Figure 5) so this observation does not necessarily demonstrate dissociation of aggregates. Quantitation of total aggregate staining shows that samples incubated with methylene blue do not have reduced levels of insoluble LC (Figure 6D). Furthermore, apparent levels of aggregated LC were higher in the precipitate fraction of all samples, consistent with retention of aggregated LC. Overall, no sample showed evidence of reduced aggregate content, consistent with their inability to prevent aggregation of similar LCs.

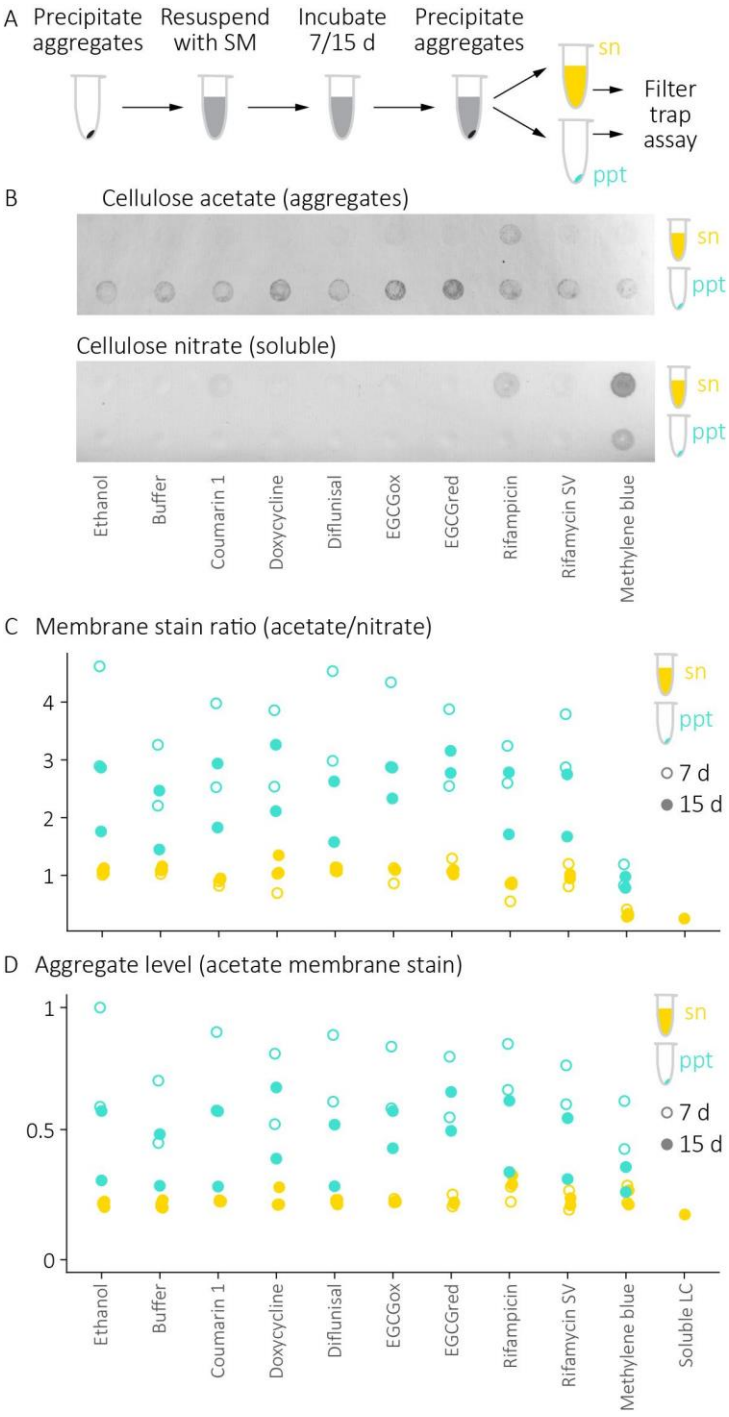

Preprints (www.preprints.org) | NOT PEER-REVIEWED | Posted: 9 April 2021 doi:10.20944/preprints202104.0270.v1

Figure 6: Dissociation of pre-formed amyloid fibrils measured by filter trap assay. (a) Experimental outline. Pre-formed fibrils (n = 2 samples per condition) were incubated with small molecules for 7 or 15 days, after which bulk aggregated LCs were precipitated by centrifugation. The soluble and insoluble LC in the supernatant (sn, orange) and precipitate (ppt, blue) were measured by filter trap assay. (b) Example membranes showing aggregated (cellulose acetate membrane stain) and soluble (cellulose nitrate membrane stain) LC in the supernatant and precipitate of one set of samples incubated for 7 days. (c) Ratio of aggregated to soluble LC after 7 days (hollow symbols) or 15 days (solid symbols). The reduced apparent aggregation observed in the presence of methylene blue appears to be due to staining of the cellulose nitrate membrane by the small molecule. (d) Total aggregate levels in each sample, relative to the most-stained membrane region.

3. Discussion

Inhibition of amyloid fibril formation is chemically challenging, and it is perhaps surprising that so many small molecules have been reported to inhibit the amyloidogenesis of several proteins in vitro or have shown efficacy in clinical trials. Table 1 summarizes the results of these experiments. None of the eight molecules investigated significantly altered LC V_L-domain aggregate formation (Figure 5) or dissolution (Figure 6) in simple assays. These data highlight the challenges involved in developing drugs for amyloid diseases. However, because AL amyloid is derived from a LC protein that is normally folded, stabilization of the LC native state presents an additional opportunity for intervention, analogous to that used successfully for transthyretin amyloidosis. The coumarin derivative that was previously identified as a stabilizer of LCs [23] was able to protect a full-length, unstable LC from unfolding and subsequent proteolysis (Figure 3). If the hypothesis that unfolding of LCs from their native state is required for aggregation is correct, molecules that stabilize LCs in a similar way to coumarin 1 could reduce aggregation and benefit patients. Importantly, although coumarin 1 is active in this assay, it has a relatively weak affinity for LCs, around 3 μM for full-length WIL, and is unlikely to be sufficiently potent to be active in vivo. Therefore, the weaker protection afforded by doxycycline (Figure 3) likely does not explain the activity of doxycycline in patients.

Preprints (www.preprints.org) | NOT PEER-REVIEWED | Posted: 9 April 2021 doi:10.20944/preprints202104.0270.v1

Molecule	**Proposed mechanism(s)**	**Stabilization of full-length WIL LC** (remaining LC, mean ± sd, n = 3)	**Suppression of JTO-V_L ThT fluorescence** (relative endpoint intensity difference vs control wells, mean ± sd, n = 3)	**Inhibition of JTO-V_L aggregation** (filter trap)	**Dissolution of 6aJL2-V_L fibrils after 15 days** (filter trap)
Coumarin 1	Native LC stabilization [23]	0.88 ± 0.13	0.97 ± 0.12	No	No
Doxycycline	Dissociation of amyloid [32] Inhibition of amyloidogenesis [33]	0.28 ± 0.037	0.94 ± 0.18	No	No
Diflunisal	Stabilizer of transthyretin (not predicted to affect LCs) [19]	0.47 ± 0.085	0.75 ± 0.08	No	No
EGCGox	Remodeling of amyloid fibrils [41,42]	0.29 ± 0.025	0.25 ± 0.01	No	No
EGCGred		0.4 ± 0.17	0.23 ± 0.02	No	No
Rifampicin	Interacts with non-native oligomers [45]	0.49 ± 0.4	0.42 ± 0.03	No	No
Rifamycin SV		0.25 ± 0.025	0.41 ± 0.11	No	No
Methylene blue	Inhibition of amyloidogenesis [46] Stabilization of LCs [25]	0.3 ± 0.057	0.41 ± 0.02	No	No

Table 1: Summary of data for each molecule.

Several studies have shown that doxycycline can suppress amyloidogenesis or disrupt amyloid fibrils in vitro. Doxycycline reduces the rate of aggregation of an amyloidogenic variant of ß2-microglobulin, as measured by both ThT fluorescence and solubility measurements [44]. However, doxycycline inhibited amyloidogenesis of 20 µM ß2-microglobulin at concentrations of 50 µM or greater. Many small molecules show activity in vitro at micromolar concentrations, but it is not clear that such activity can be extrapolated to patients, where drug absorption and plasma protein binding

can significantly reduce the effective concentration of the small molecule, even if toxicity is not limiting. A small, uncontrolled clinical trial suggested improvements in patients [55] with ß2-microglobulin amyloidosis, even though the plasma concentration of doxycycline in these individuals was only around 2 µM. Another study showed that doxycycline reduced fibril deposition in a mouse model of AL amyloidosis [34] and inhibited amyloid formation, but not aggregation, of a full-length LC derived from the *IGKV1-33* gene. The experimental conditions used to induce aggregation of this full-length LC included cycles of 4-hour incubations at 65 °C. Doxycycline was also observed to alter the morphology of fibrils extracted from an individual with AL amyloidosis [34]. These observations are consistent with data presented in Figures 5 and 6 because alternative aggregate species would still be detected in the filter trap assays. Overall, the data presented here are consistent with a mechanism of action for doxycycline in AL amyloidosis that does not depend entirely on its ability to prevent amyloidogenesis or disrupt fibrils. Thus, doxycycline may complement novel, non-cytotoxic therapies in patients.

Small molecules can interfere with biochemical or cell-based assays in multiple ways. Several classes of molecules are regarded as “pan-assay interference” compounds, or PAINS. EGCG is a well-known example: catechols can form reactive orthoquinones upon oxidation [42]. However, pre-oxidation of EGCG did not alter its activity in these assays. Methylene blue, rifamycin SV and rifampicin all appear to reduce the fluorescence of amyloid-bound ThT. Each of these molecules is colored in solution, a property that should be noted as a potential complication in any optical assay.

The major limitation of this study is that I only considered single examples of LCs in each assay. The effects of individual molecules could be unique to specific LC sequences studied. Notably, the study which identified methylene blue as a stabilizer of LCs investigated its binding to the V_L-domain of a LC derived from the *IGLV2-8* gene [25]. However, the *IGLV6-57* LC gene used in these experiments is over-represented in AL amyloidosis compared to the normal repertoire [47]. I did not investigate whether small molecules could alter the structural properties of LC aggregates because the physiological relevance of different aggregate structures is not known. Non-amyloid LC aggregates are associated with organ toxicity in light chain deposition disease and the structures of the three LC amyloid fibrils determined at high resolution are distinct.

Treatment of AL amyloidosis has benefited enormously from improvements in cytotoxic drugs directed against clonal plasma cells over the last three decades [1]. Further improvements in patient care may be possible by augmenting this strategy with drugs that target different aspects of the disease pathology.

Preprints (www.preprints.org) | NOT PEER-REVIEWED | Posted: 9 April 2021 doi:10.20944/preprints202104.0270.v1

4. Materials and methods

Small molecules were purchased from Sigma or Thermo Fisher (Acros Organics). 5 mM stocks in water (doxycycline hyclate, EGCG, methylene blue) or ethanol (coumarin 1, diflunisal, rifamycin SV, rifampicin) were prepared and stored at -20 °C until needed. “Oxidized” EGCG was prepared by incubating aliquots of EGCG overnight at 37 °C in water, which were then stored at -20 °C. All experiments were carried out in phosphate buffered saline (PBS; 1.5 mM KH_2PO_4, 8.1 mM Na_2HPO_4, 2.7 mM KCl, 138 mM NaCl, pH 7.4) at 37 °C.

Data were analyzed and figures prepared using the “Tidyverse” [56] suite of tools for R [57], within the RStudio environment [58]. Final figures were prepared using Adobe Acrobat.

4.1. Light chain preparation

Light chains were cloned into vectors containing T7 promoters and recombinantly expressed in BL21 (DE3) *E. coli* as previously described [9]. Full-length LCs were expressed as inclusion bodies in the *E. coli* cytosol. Cells were lysed by sonication and insoluble material was washed three times with PBS containing 1% NP-40 detergent then once with PBS. Inclusion bodies were resuspended in 25 mM Tris-Cl, pH 8 (room temperature pH value) containing 4 M guanidine hydrochloride and 5 mM dithiothreitol for at least 2 hours at 4 °C, before being refolded by dropwise dilution into 25 mM Tris-Cl pH 8 on ice to dilute out the denaturant. V_L-domains were expressed in the E. coli periplasm and extracted by periplasmic shock. Cell pellets were resuspended in 200 mM tris pH 8 containing 0.5 M sucrose and 5 mM EDTA, incubated on ice for 30 minutes, then shocked by addition of two volumes of deionized water. Cells were removed by centrifugation. Both full-length LCs and VL-domains were concentrated by ammonium sulfate fractionation (LCs precipitate in the 25-75% saturation fraction at 4 °C), resuspended in 25 mM Tris-Cl, pH 8, and dialysed against 25 mM Tris-Cl, pH 8 to remove residual ammonium sulfate. LCs were purified by ion exchange and size exclusion chromatography on Source 15Q and Superdex 75 columns (GE Life Sciences). LCs were eluted from the size exclusion column in PBS, aliquoted, snap-frozen and stored at -80 °C.

4.2. Limited proteolysis

LCs (5 µM) were incubated at 37 °C for 4 hours in the presence of small molecules (50 µM) or appropriate vehicle control, with or without 200 nM proteinase K (Thermo Fisher). Reactions were initiated by adding 2 µl proteinase K or buffer to 18 µl LC solution and incubated in a thermocycler with a heated lid to minimize evaporation. At the end of the incubation time, reactions were quenched with 2 µl of 10 mM phenylmethyl sulfonyl fluoride, which rapidly and irreversibly inactivates the protease. The extent of proteolysis was measured by SDS-PAGE. Loading buffer

Preprints (www.preprints.org) | NOT PEER-REVIEWED | Posted: 9 April 2021 doi:10.20944/preprints202104.0270.v1

was added to each sample to a final concentration of 2% SDS, 10% glycerol and 0.1% 2-mercaptoethanol and the samples were incubated at 98 °C for 6 minutes. Samples were run on 16% tris-glycine polyacrylamide gels (Thermo Fisher), stained with GelCode Blue (Thermo Fisher) and visualized using an ImageQuant LAS 4000 gel imaging system (GE Life Sciences). Bands were quantitated with ImageLab software (BioRad). Remaining LC was defined as the intensity of the full-length LC band after proteolysis, relative to the unproteolyzed LC sample, calculated independently for each of three gels.

4.3. Amyloidogenesis kinetics

Thioflavin T (Sigma) was dissolved in ethanol, diluted in PBS to approximately 200 µM, then filtered to remove aggregates. Filtration of ThT often leads to some loss of dye, so ThT concentration was determined by spectroscopy (extinction coefficient of 28000 at 414 nm) after filtration. Aggregation was carried out in black, clear-bottomed polystyrene microwell plates (Corning #3631). JTO-VL was thawed and filtered through a 0.22 µm syringe filter, then added to pre-filtered ThT at final concentrations of 5 µM LC and 5 µM ThT in PBS. The outer wells of the plate were filled with 200 µl PBS to help stabilize the temperature and humidity within the sealed plate and thereby minimize evaporation, leaving 60 wells for LC samples. To each of these wells, 99 µl of LC and ThT solution was added, followed by 1 µl of the appropriate small molecule or vehicle. Small molecule was added to 3 wells per molecule before aggregation, and a further 3 wells were used as controls where the small molecule was added after aggregation to assess the effect of the molecule on ThT fluorescence. Plates were sealed with film, then covered with a lid that was held in place by tape. Fluorescence (λex = 440 nm, λem = 480 nm, reading through the bottom of the plate) was measured in a SpectraMax M5 platereader (Molecular Devices).The plates were incubated quiescently at 37 °C for 10 minutes to allow the reactions to equilibrate, then an initial reading was taken. Plates were incubated at 37 °C on an orbital plate shaker operating at 1000 rpm. Further readings were taken at regular intervals.

Once aggregation had completed (determined by a plateau in the ThT fluorescence) in all wells without added small molecule, a final fluorescence measurement was taken. The plate was then unsealed and a 1 µl bolus of small molecule solution was added to each of the 3 control wells. Fluorescence was measured again to determine the effect of small molecule on ThT fluorescence. The change in fluorescence upon small molecule addition was defined as the difference in fluorescence in each control well, corrected for the average change in the wells which had initially contained the same small molecule, which had not otherwise been manipulated between readings.

Preprints (www.preprints.org) | NOT PEER-REVIEWED | Posted: 9 April 2021 doi:10.20944/preprints202104.0270.v1

4.4. Filter trap assay

Samples were drawn through a cellulose acetate membrane (Sterilitech) and cellulose nitrate membrane (Bio-Rad) using a Bio-Dot vacuum manifold (Boi-Rad). The membranes were pre-wetted with PBS, then 100 µl of sample was drawn through. The protein spots were washed 3 times by drawing 200 µl PBS through the membranes. Membranes were stained with 0.1% (w/v) amido black in 10% (v/v) acetic acid, then gently washed with 5% acetic acid and deionized water until the background stain was removed. Spots were imaged using an ImageQuant LAS 4000 gel imaging system (GE Life Sciences) and quantitated with ImageLab software (BioRad), treating each spot as a gel band in order to control the software's background subtraction feature. The ratios between the background-corrected intensities are reported in Figure 5 and 6 without further normalization.

4.5. Fibril dissociation

A single batch of 6aJL2-VL fibrils was prepared by incubating 5 µM VL-domain in PBS at 37 °C, 200 rpm until visible aggregates formed. Fibrils were vortexed, then split into 500 µl aliquots and centrifuged at 20,000 g for 10 min. The supernatant was aspirated to remove any remaining soluble LC, leaving 10 µl in the tubes to avoid disturbing the pelleted fibrils. The fibrils were resuspended in PBS containing 50 µM small molecule and vortexed. Four samples per molecule were incubated quiescently at 37 °C for 7 or 15 days (2 samples each). The 15-day incubation was chosen to replicate similar experiments where doxycycline was observed to dissociate fibrils [32]. After incubation, samples were centrifuged at 20,000 g for 10 min to separate soluble LC from fibrils. The pellets were resuspended in PBS without small molecules and both samples were stored at 4 °C until soluble and insoluble fractions were measured by filter trap assay, which was carried out as described above. A total of 80 samples was used for the filter trap assay: two replicates each of supernatant and precipitate, at two timepoints, for ten small molecules including ethanol and water vehicles. This experimental design precluded triplicate experiments, so that all samples could be stained on the same membranes.

Acknowledgements

I thank members of the Boston University Amyloidosis Center for helpful discussions. This work was supported by the Charles J. Brown Amyloid Center Research Fund of the Amyloidosis Center, Boston University School of Medicine.

Conflict of interest statement

I am a co-inventor on a patent (WO/2020/205683) held by Scripps Research that describes the use of small molecules as stabilizer drugs for AL amyloidosis. The funders had no role in the design of the study; in the collection, analyses, or interpretation of data; in the writing of the manuscript, or in the decision to publish the results.

References

1. Merlini, G.; Dispenzieri, A.; Sanchorawala, V.; Schönland, S.O.; Palladini, G.; Hawkins, P.N.; Gertz, M.A. Systemic immunoglobulin light chain amyloidosis. *Nat Rev Dis Primers* **2018**, *4*, 38, doi:10.1038/s41572-018-0034-3.
2. Morgan, G.J.; Wall, J.S. The Process of Amyloid Formation due to Monoclonal Immunoglobulins. *Hematol. Oncol. Clin. North Am.* **2020**, *34*, 1041–1054, doi:10.1016/j.hoc.2020.07.003.
3. Benson, M.D.; Buxbaum, J.N.; Eisenberg, D.S.; Merlini, G.; Saraiva, M.J.M.; Sekijima, Y.; Sipe, J.D.; Westermark, P. Amyloid nomenclature 2020: update and recommendations by the International Society of Amyloidosis (ISA) nomenclature committee. *Amyloid* **2020**, *27*, 217–222, doi:10.1080/13506129.2020.1835263.
4. Wechalekar, A.D.; Gillmore, J.D.; Hawkins, P.N. Systemic amyloidosis. *Lancet* **2015**, doi:10.1016/S0140-6736(15)01274-X.
5. Palladini, G.; Milani, P.; Merlini, G. Management of AL amyloidosis in 2020. *Blood* **2020**, *136*, 2620–2627, doi:10.1182/blood.2020006913.
6. Sanchorawala, V.; Sarosiek, S.; Schulman, A.; Mistark, M.; Migre, M.E.; Cruz, R.; Sloan, J.M.; Brauneis, D.; Shelton, A.C. Safety, Tolerability, and Response Rates of Daratumumab in Relapsed AL Amyloidosis: Results of a Phase II Study. *Blood* **2020**, doi:10.1182/blood.2019004436.
7. Muchtar, E.; Gertz, M.A.; Kumar, S.K.; Lacy, M.Q.; Dingli, D.; Buadi, F.K.; Grogan, M.; Hayman, S.R.; Kapoor, P.; Leung, N.; et al. Improved outcomes for newly diagnosed AL amyloidosis between 2000 and 2014: cracking the glass ceiling of early death. *Blood* **2017**, *129*, 2111–2119, doi:10.1182/blood-2016-11-751628.
8. Milani, P.; Merlini, G.; Palladini, G. Novel Therapies in Light Chain Amyloidosis. *Kidney Int Rep* **2018**, *3*, 530–541, doi:10.1016/j.ekir.2017.11.017.
9. Morgan, G.J.; Kelly, J.W. The Kinetic Stability of a Full-Length Antibody Light Chain Dimer Determines whether Endoproteolysis Can Release Amyloidogenic Variable Domains. *J. Mol. Biol.* **2016**, *428*, 4280–4297, doi:10.1016/j.jmb.2016.08.021.
10. Buxbaum, J. Mechanisms of disease: monoclonal immunoglobulin deposition. Amyloidosis, light chain deposition disease, and light and heavy chain deposition disease. *Hematol. Oncol. Clin. North Am.* **1992**, *6*, 323–346.
11. Blancas-Mejía, L.M.; Horn, T.J.; Marin-Argany, M.; Auton, M.; Tischer, A.; Ramirez-Alvarado, M. Thermodynamic and fibril formation studies of full length immunoglobulin light chain AL-09 and its germline protein using scan rate dependent thermal unfolding. *Biophys. Chem.* **2015**, *207*, 13–20, doi:10.1016/j.bpc.2015.07.005.
12. Swuec, P.; Lavatelli, F.; Tasaki, M.; Paissoni, C.; Rognoni, P.; Maritan, M.; Brambilla, F.; Milani, P.; Mauri, P.; Camilloni, C.; et al. Cryo-EM structure of cardiac amyloid fibrils from an immunoglobulin light chain AL amyloidosis patient. *Nat. Commun.* **2019**, *10*, 1269, doi:10.1038/s41467-019-09133-w.
13. Radamaker, L.; Baur, J.; Huhn, S.; Haupt, C.; Hegenbart, U.; Schönland, S.; Bansal, A.; Schmidt, M.; Fändrich, M. Cryo-EM reveals structural breaks in a patient-derived amyloid fibril from systemic AL amyloidosis. *Nat. Commun.* **2021**, *12*, 875, doi:10.1038/s41467-021-21126-2.

14. Radamaker, L.; Lin, Y.-H.; Annamalai, K.; Huhn, S.; Hegenbart, U.; Schönland, S.O.; Fritz, G.; Schmidt, M.; Fändrich, M. Cryo-EM structure of a light chain-derived amyloid fibril from a patient with systemic AL amyloidosis. *Nat. Commun.* **2019**, *10*, 1103, doi:10.1038/s41467-019-09032-0.
15. Enqvist, S.; Sletten, K.; Westermark, P. Fibril protein fragmentation pattern in systemic AL-amyloidosis. *J. Pathol.* **2009**, *219*, 473–480, doi:10.1002/path.2607.
16. Lavatelli, F.; Mazzini, G.; Ricagno, S.; Iavarone, F.; Rognoni, P.; Milani, P.; Nuvolone, M.; Swuec, P.; Caminito, S.; Tasaki, M.; et al. Mass spectrometry characterization of light chain fragmentation sites in cardiac AL amyloidosis:insights into the timing of proteolysis. *J. Biol. Chem.* **2020**, doi:10.1074/jbc.RA120.013461.
17. Maurer, M.S.; Schwartz, J.H.; Gundapaneni, B.; Elliott, P.M.; Merlini, G.; Waddington-Cruz, M.; Kristen, A.V.; Grogan, M.; Witteles, R.; Damy, T.; et al. Tafamidis Treatment for Patients with Transthyretin Amyloid Cardiomyopathy. *N. Engl. J. Med.* **2018**, *379*, 1007–1016, doi:10.1056/NEJMoa1805689.
18. Bulawa, C.E.; Connelly, S.; Devit, M.; Wang, L.; Weigel, C.; Fleming, J. a.; Packman, J.; Powers, E.T.; Wiseman, R.L.; Foss, T.R.; et al. Tafamidis, a potent and selective transthyretin kinetic stabilizer that inhibits the amyloid cascade. *Proc. Natl. Acad. Sci. U. S. A.* **2012**, *109*, 9629–9634, doi:10.1073/pnas.1121005109.
19. Miller, S.R.; Sekijima, Y.; Kelly, J.W. Native state stabilization by NSAIDs inhibits transthyretin amyloidogenesis from the most common familial disease variants. *Lab. Invest.* **2004**, *84*, 545–552, doi:10.1038/labinvest.3700059.
20. Berk, J.L.; Suhr, O.B.; Obici, L.; Sekijima, Y.; Zeldenrust, S.R.; Yamashita, T.; Heneghan, M.A.; Gorevic, P.D.; Litchy, W.J.; Wiesman, J.F.; et al. Repurposing Diflunisal for Familial Amyloid Polyneuropathy: A Randomized Clinical Trial. *JAMA* **2013**, *310*, 2658–2667, doi:10.1001/jama.2013.283815.
21. Sant'Anna, R.; Gallego, P.; Robinson, L.Z.; Pereira-Henriques, A.; Ferreira, N.; Pinheiro, F.; Esperante, S.; Pallares, I.; Huertas, O.; Almeida, M.R.; et al. Repositioning tolcapone as a potent inhibitor of transthyretin amyloidogenesis and associated cellular toxicity. *Nat. Commun.* **2016**, *7*, 10787, doi:10.1038/ncomms10787.
22. Penchala, S.C.; Connelly, S.; Wang, Y.; Park, M.S.; Zhao, L.; Baranczak, A.; Rappley, I.; Vogel, H.; Liedtke, M.; Witteles, R.M.; et al. AG10 inhibits amyloidogenesis and cellular toxicity of the familial amyloid cardiomyopathy-associated V122I transthyretin. *Proc. Natl. Acad. Sci. U. S. A.* **2013**, *110*, 9992–9997, doi:10.1073/pnas.1300761110.
23. Morgan, G.J.; Yan, N.L.; Mortenson, D.E.; Rennella, E.; Blundon, J.M.; Gwin, R.M.; Lin, C.-Y.; Stanfield, R.L.; Brown, S.J.; Rosen, H.; et al. Stabilization of amyloidogenic immunoglobulin light chains by small molecules. *Proc. Natl. Acad. Sci. U. S. A.* **2019**, *116*, 8360–8369, doi:10.1073/pnas.1817567116.
24. Yan, N.L.; Santos-Martins, D.; Rennella, E.; Sanchez, B.B.; Chen, J.S.; Kay, L.E.; Wilson, I.A.; Morgan, G.J.; Forli, S.; Kelly, J.W. Structural basis for the stabilization of amyloidogenic immunoglobulin light chains by hydantoins. *Bioorg. Med. Chem. Lett.* **2020**, *30*, 127356, doi:10.1016/j.bmcl.2020.127356.
25. Brumshtein, B.; Esswein, S.R.; Salwinski, L.; Phillips, M.L.; Ly, A.T.; Cascio, D.; Sawaya, M.R.; Eisenberg, D.S. Inhibition by small-molecule ligands of formation of amyloid fibrils of an immunoglobulin light chain variable domain. *Elife* **2015**, *4*, doi:10.7554/eLife.10935.
26. Tóth, G.; Gardai, S.J.; Zago, W.; Bertoncini, C.W.; Cremades, N.; Roy, S.L.; Tambe, M.A.; Rochet, J.-C.; Galvagnion, C.; Skibinski, G.; et al. Targeting the intrinsically disordered structural ensemble of α-synuclein by small molecules as a potential therapeutic strategy for Parkinson's disease. *PLoS One* **2014**, *9*, e87133, doi:10.1371/journal.pone.0087133.
27. Sievers, S.A.; Karanicolas, J.; Chang, H.W.; Zhao, A.; Jiang, L.; Zirafi, O.; Stevens, J.T.; Münch, J.; Baker, D.; Eisenberg, D. Structure-based design of non-natural amino-acid inhibitors of amyloid fibril formation. *Nature* **2011**, *475*, 96–100, doi:10.1038/nature10154.
28. Gertz, M.A.; Cohen, A.D.; Comenzo, R.L.; Du Mond, C.; Kastritis, E.; Landau, H.J.; Libby, E.N., III; Liedtke, M.; Merlini, G.; Sanchorawala, V.; et al. Results of the Phase 3 VITAL study of NEOD001 (birtamimab) plus standard of care in patients with light chain (AL) amyloidosis suggest survival benefit for Mayo stage IV patients. *Blood* **2019**, *134*, 3166–3166,

doi:10.1182/blood-2019-124482.
29. Edwards, C.V.; Bhutani, D.; Mapara, M.; Radhakrishnan, J.; Shames, S.; Maurer, M.S.; Leng, S.; Wall, J.S.; Solomon, A.; Eisenberger, A.; et al. One year follow up analysis of the phase 1a/b study of chimeric fibril-reactive monoclonal antibody 11-1F4 in patients with AL amyloidosis. *Amyloid* **2019**, *26*, 115–116, doi:10.1080/13506129.2019.1584892.
30. Richards, D.B.; Cookson, L.M.; Barton, S.V.; Liefaard, L.; Lane, T.; Hutt, D.F.; Ritter, J.M.; Fontana, M.; Moon, J.C.; Gillmore, J.D.; et al. Repeat doses of antibody to serum amyloid P component clear amyloid deposits in patients with systemic amyloidosis. *Sci. Transl. Med.* **2018**, *10*, doi:10.1126/scitranslmed.aan3128.
31. Richards, D.B.; Cookson, L.M.; Berges, A.C.; Barton, S.V.; Lane, T.; Ritter, J.M.; Fontana, M.; Moon, J.C.; Pinzani, M.; Gillmore, J.D.; et al. Therapeutic Clearance of Amyloid by Antibodies to Serum Amyloid P Component. *N. Engl. J. Med.* **2015**, *373*, 1106–1114, doi:10.1056/NEJMoa1504942.
32. Cardoso, I.; Merlini, G.; Saraiva, M.J. 4’-iodo-4'-deoxydoxorubicin and tetracyclines disrupt transthyretin amyloid fibrils in vitro producing noncytotoxic species: screening for TTR fibril disrupters. *FASEB J.* **2003**, *17*, 803–809, doi:10.1096/fj.02-0764com.
33. Giorgetti, S.; Raimondi, S.; Pagano, K.; Relini, A.; Bucciantini, M.; Corazza, A.; Fogolari, F.; Codutti, L.; Salmona, M.; Mangione, P.; et al. Effect of tetracyclines on the dynamics of formation and destructuration of beta2-microglobulin amyloid fibrils. *J. Biol. Chem.* **2011**, *286*, 2121–2131, doi:10.1074/jbc.M110.178376.
34. Ward, J.E.; Ren, R.; Toraldo, G.; Soohoo, P.; Guan, J.; O’Hara, C.; Jasuja, R.; Trinkaus-Randall, V.; Liao, R.; Connors, L.H.; et al. Doxycycline reduces fibril formation in a transgenic mouse model of AL amyloidosis. *Blood* **2011**, *118*, 6610–6617, doi:10.1182/blood-2011-04-351643.
35. Faravelli, G.; Raimondi, S.; Marchese, L.; Partridge, F.A.; Soria, C.; Mangione, P.P.; Canetti, D.; Perni, M.; Aprile, F.A.; Zorzoli, I.; et al. C. elegans expressing D76N β2-microglobulin: a model for in vivo screening of drug candidates targeting amyloidosis. *Sci. Rep.* **2019**, *9*, 19960, doi:10.1038/s41598-019-56498-5.
36. D’Souza, A.; Szabo, A.; Flynn, K.E.; Dhakal, B.; Chhabra, S.; Pasquini, M.C.; Weihrauch, D.; Hari, P.N. Adjuvant doxycycline to enhance anti-amyloid effects: Results from the dual phase 2 trial. *EClinicalMedicine* **2020**, *23*, 100361, doi:10.1016/j.eclinm.2020.100361.
37. Wechalekar, A.; Whelan, C.; Lachmann, H.; Fontana, M.; Mahmood, S.; Gillmore, J.D.; Hawkins, P.N. Oral Doxycycline Improves Outcomes of Stage III AL Amyloidosis - a Matched Case Control Study. *Blood* **2015**, *126*, 732–732, doi:10.1182/blood.V126.23.732.732.
38. Kumar, S.K.; Dispenzieri, A.; Lacy, M.Q.; Hayman, S.R.; Buadi, F.K.; Dingli, D.; Zeldenrust, S.R.; Ramirez-Alvarado, M.; Kapoor, P.; Hogan, W.; et al. Doxycycline Used As Post Transplant Antibacterial Prophylaxis Improves Survival in Patients with Light Chain Amyloidosis Undergoing Autologous Stem Cell Transplantation. *Blood* **2012**, *120*, 3138–3138.
39. Solis, G.M.; Kardakaris, R.; Valentine, E.R.; Bar-Peled, L.; Chen, A.L.; Blewett, M.M.; McCormick, M.A.; Williamson, J.R.; Kennedy, B.; Cravatt, B.F.; et al. Translation attenuation by minocycline enhances longevity and proteostasis in old post-stress-responsive organisms. *Elife* **2018**, *7*, e40314, doi:10.7554/eLife.40314.
40. Castro, M.M.; Kandasamy, A.D.; Youssef, N.; Schulz, R. Matrix metalloproteinase inhibitor properties of tetracyclines: therapeutic potential in cardiovascular diseases. *Pharmacol. Res.* **2011**, *64*, 551–560, doi:10.1016/j.phrs.2011.05.005.
41. Andrich, K.; Hegenbart, U.; Kimmich, C.; Kedia, N.; Bergen, H.R., Rd; Schönland, S.; Wanker, E.; Bieschke, J. Aggregation of Full-length Immunoglobulin Light Chains from Systemic Light Chain Amyloidosis (AL) Patients Is Remodeled by Epigallocatechin-3-gallate. *J. Biol. Chem.* **2017**, *292*, 2328–2344, doi:10.1074/jbc.M116.750323.
42. Palhano, F.L.; Lee, J.; Grimster, N.P.; Kelly, J.W. Toward the molecular mechanism(s) by which EGCG treatment remodels mature amyloid fibrils. *J. Am. Chem. Soc.* **2013**, *135*, 7503–7510, doi:10.1021/ja3115696.
43. Meshitsuka, S.; Shingaki, S.; Hotta, M.; Goto, M.; Kobayashi, M.; Ukawa, Y.; Sagesaka, Y.M.; Wada, Y.; Nojima, M.; Suzuki, K. Phase 2 trial of daily, oral epigallocatechin gallate in patients with light-chain amyloidosis. *Int. J. Hematol.* **2017**, *105*, 295–308, doi:10.1007/s12185-016-

2112-1.
44. Raimondi, S.; Porcari, R.; Mangione, P.P.; Verona, G.; Marcoux, J.; Giorgetti, S.; Taylor, G.W.; Ellmerich, S.; Ballico, M.; Zanini, S.; et al. A specific nanobody prevents amyloidogenesis of D76N β2-microglobulin in vitro and modifies its tissue distribution in vivo. *Sci. Rep.* **2017**, *7*, 46711, doi:10.1038/srep46711.
45. Woods, L. a.; Platt, G.W.; Hellewell, A.L.; Hewitt, E.W.; Homans, S.W.; Ashcroft, A.E.; Radford, S.E. Ligand binding to distinct states diverts aggregation of an amyloid-forming protein. *Nat. Chem. Biol.* **2011**, *7*, 730–739, doi:10.1038/nchembio.635.
46. Soeda, Y.; Saito, M.; Maeda, S.; Ishida, K.; Nakamura, A.; Kojima, S.; Takashima, A. Methylene Blue Inhibits Formation of Tau Fibrils but not of Granular Tau Oligomers: A Plausible Key to Understanding Failure of a Clinical Trial for Alzheimer's Disease. *J. Alzheimers. Dis.* **2019**, *68*, 1677–1686, doi:10.3233/JAD-181001.
47. Bodi, K.; Prokaeva, T.; Spencer, B.; Eberhard, M.; Connors, L.H.; Seldin, D.C. AL-Base: a visual platform analysis tool for the study of amyloidogenic immunoglobulin light chain sequences. *Amyloid* **2009**, *16*, 1–8, doi:10.1080/13506120802676781.
48. Park, C.; Marqusee, S. Pulse proteolysis: a simple method for quantitative determination of protein stability and ligand binding. *Nat. Methods* **2005**, *2*, 207–212, doi:10.1038/nmeth740.
49. Wall, J.; Schell, M.; Murphy, C.; Hrncic, R.; Stevens, F.J.; Solomon, A. Thermodynamic instability of human lambda 6 light chains: correlation with fibrillogenicity. *Biochemistry* **1999**, *38*, 14101–14108, doi:10.1021/bi991131j.
50. Rennella, E.; Morgan, G.J.; Yan, N.; Kelly, J.W.; Kay, L.E. The Role of Protein Thermodynamics and Primary Structure in Fibrillogenesis of Variable Domains from Immunoglobulin Light Chains. *J. Am. Chem. Soc.* **2019**, *141*, 13562–13571, doi:10.1021/jacs.9b05499.
51. Rennella, E.; Morgan, G.J.; Kelly, J.W.; Kay, L.E. Role of domain interactions in the aggregation of full-length immunoglobulin light chains. *Proc. Natl. Acad. Sci. U. S. A.* **2019**, *116*, 854–863, doi:10.1073/pnas.1817538116.
52. Wanker, E.E.; Scherzinger, E.; Heiser, V.; Sittler, A.; Eickhoff, H.; Lehrach, H. Membrane filter assay for detection of amyloid-like polyglutamine-containing protein aggregates. *Methods Enzymol.* **1999**, *309*, 375–386.
53. Harper, S.; Speicher, D.W. Detection of proteins on blot membranes. *Curr. Protoc. Protein Sci.* **2001**, *Chapter 10*, Unit 10.8, doi:10.1002/0471140864.ps1008s00.
54. Blancas-Mejia, L.M.; Tellez, L.A.; del Pozo-Yauner, L.; Becerril, B.; Sanchez-Ruiz, J.M.; Fernandez-Velasco, D.A. Thermodynamic and kinetic characterization of a germ line human lambda6 light-chain protein: the relation between unfolding and fibrillogenesis. *J. Mol. Biol.* **2009**, *386*, 1153–1166, doi:10.1016/j.jmb.2008.12.069.
55. Montagna, G.; Cazzulani, B.; Obici, L.; Uggetti, C.; Giorgetti, S.; Porcari, R.; Ruggiero, R.; Mangione, P.P.; Brambilla, M.; Lucchetti, J.; et al. Benefit of doxycycline treatment on articular disability caused by dialysis related amyloidosis. *Amyloid* **2013**, *20*, 173–178, doi:10.3109/13506129.2013.803463.
56. Wickham, H.; Averick, M.; Bryan, J.; Chang, W.; McGowan, L.D.; François, R.; Grolemund, G.; Hayes, A.; Henry, L.; Hester, J.; et al. Welcome to the tidyverse. *Journal of Open Source Software* 2019, *4*, 1686.
57. R Core Team R: A Language and Environment for Statistical Computing Available online: https://www.R-project.org/.
58. RStudio Team RStudio: Integrated Development Environment for R 2020.